

Water-column geochemical anomalies associated with the remnants of a mega plume: A case study after CR-2003 hydrothermal event in Carlsberg Ridge, NW Indian Ocean

Durbar Ray¹, Imran H. Mirza¹, L. Surya Prakash¹, Sujata Kaisary^{1,*}, Y. V. B. Sarma^{1,2}, B. R. Rao¹, Y. K. Somayajulu¹, R. K. Drolia³ and K. A. Kamesh Raju¹

¹National Institute of Oceanography, Goa 403 004, India

²Present address: Sultan Qaboos University, Muscat, Oman

³National Geophysical Research Institute, Hyderabad 500 007, India

Recently, an unusually large hydrothermal event (CR-2003) was reported over the slow-spreading Carlsberg Ridge between 05°41'N, 61°30'E and 06°20'N, 60°33'E. To investigate the after effects (if any) of such a large-scale emission, almost a year later in July 2004, the water column along the 50 km ridge segment was surveyed. Results show that while the thermal and optical signatures have largely reduced with time, the chemical signatures do persist between 2500 and 2900 m. Geochemical features like Fe/Mn, Mn/heat ratios, characteristic of event plume, also show major changes. Distribution of dissolved manganese, methane, helium-3 and suspended particulates further down the water column was indicative of one more plume layer between 3150 and 3400 m. The high volatile and less particulate metal content of the deep layer points towards a relatively fresh event.

Keywords: Carlsberg Ridge, geochemical anomalies, hydrothermal event plume, water column.

ACTIVE hydrothermal vents with continuous emission are well known in the world mid-oceanic ridge system, but cataclysmic mega events which release voluminous solution within a short period of time are rare in the deep sea. The major fluxes of heat, volatiles and trace elements associated with sudden emission of any event plume slowly mix with the large volume of ambient sea water and possess a long-term effect on the local water body. Although sea water has enough buffering capacity, a large-scale event could produce a significant change in deep oceanic biogeochemistry. Deep sea water in close contact with hydrothermal fluid shows enrichment (due to hydrothermal supply) or depletion (through scavenging during hydrothermal precipitation) of certain chemical components. As

the plume proceeds, it mixes with deep sea water and reduced chemical components of hydrothermal origin become oxidized away from the source. Immediately after emission, iron changes phase from dissolved to particulate mostly through Fe (II) oxidation and colloid aggregation following a pseudo first-order and second order kinetics respectively¹. Thus with plume ageing, particulate iron (%PFe) increases and thus dissolved iron is eliminated faster than quasi-conservative manganese away from the source. Besides this, volatile (methane, helium-3) content and ratio of dissolved Fe/Mn, Mn/heat and CH₄/Mn are also useful to analyse certain geochemical aspects of a plume. The oxidative particulates make plume waters turbid and this turbidity in turn can be detected with optical sensors mounted on a CTD or attached to deep tow. The optical backscatter profiles along with dissolved manganese signatures help to detect the spatial distribution of a plume over time.

In June 2003 a large-scale event plume, CR-2003 was reported over Carlsberg Ridge (CR), NW Indian Ocean². Recently, Murton *et al.*³ have reported that the CR-2003 event was one of the largest ever recorded in world oceans, specially in terms of total heat liberated ($75-240 \times 10^{15}$ J), thickness (> 700 m), lateral extension (> 70 km) and raising height (1400 m) of plume. One year after the discovery of the CR-2003 event plume, we visited the same site (NW CR) to study the long-term consequences, if any, of that mega event. During our cruise (SK-207) on-board *ORV Sagar Kanya*, we found anomalous chemical signatures in certain depth ranges in the water column and these have been presented here.

Tectonic setting

The CR is the north and northwestern portion of the Indian ridge system and forms the accreting plate boundary between the Somalia-India and Arabia-Somalia plates. The

*For correspondence. (e-mail: sujata@nio.org)

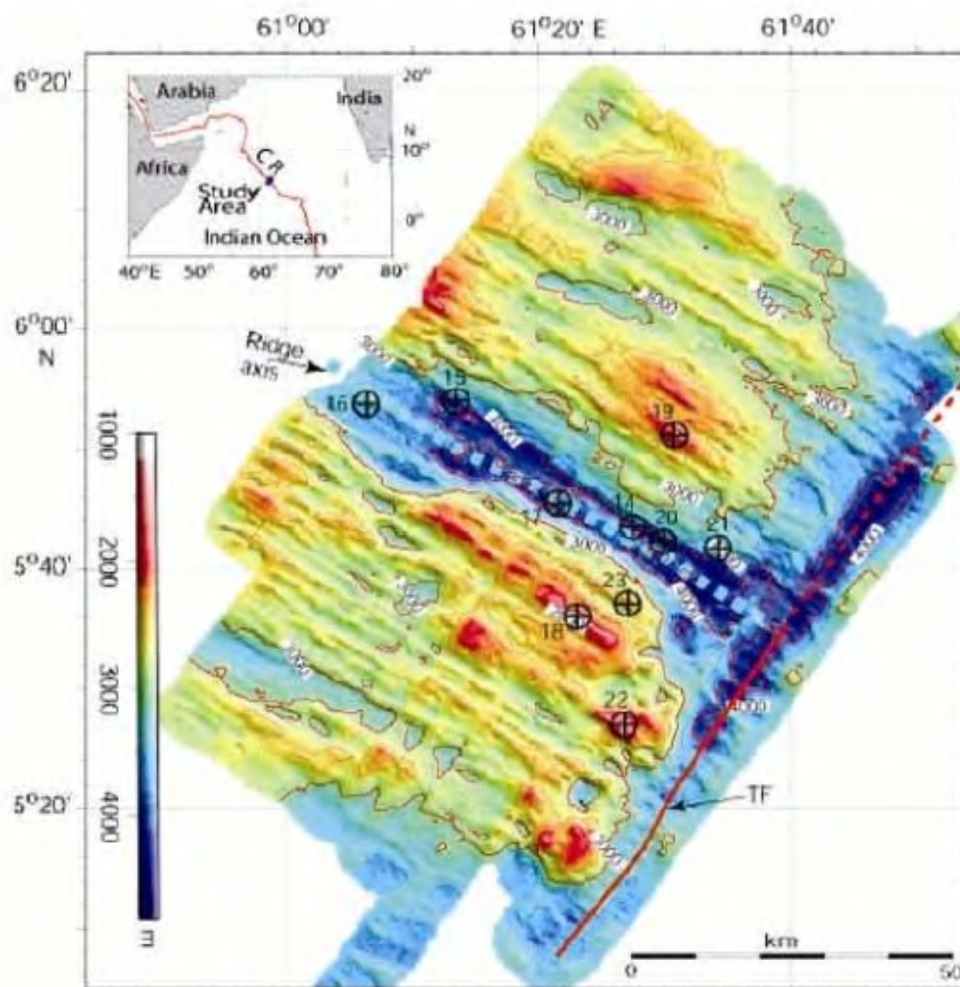


Figure 1. Sea-floor topography generated from swath bathymetry of survey area along with CTD hydrocast locations on Carlsberg Ridge. Spreading centre and transform fault (TF) are marked with contour interval of 500 m.

Owen Fracture Zone offsets the CR by about 350 km forming the transform boundary between the Arabian and Indian plates at the Somalia–Arabian–Indian triple junction⁴. The ridge exhibits typical slow-spreading morphology, with a well-defined rift valley and slow-spreading rates.

An 80-km long segment over the CR has been mapped by swath bathymetry with 100% insonification and off-axis coverage of about 50 km on either side of the spreading centre. The CR displays striking similarities with parts of the Mid-Atlantic Ridge in terms of spreading rate and morphology. While there are not many geophysical studies on this segment using modern tools, studies carried out by Chaubey *et al.*⁵ and Ramana *et al.*⁶ give a brief idea about the tectonic setting of the ridge segment. Previous investigations^{6,7} revealed that the half spreading rates for the CR segments, recorded in the oceanic crust magnetization, varied from 12 to 16 mm/yr.

The high-resolution swath bathymetry (Figure 1) of the study area shows typical slow-spreading ridge morphology characterized by a deep rift valley with steep walls. The ridge segment is bounded on the southeast by a right-lateral transform fault. The valley floor lies at about 4000 m depth and the width varies between 8 and 12 km, narrow and shallow at the segment centre and wider and deeper towards the ridge–transform intersection. The western off-axis floor is characterized by a well-defined inside corner high with a minimum depth of about 1400 m at the ridge–transform intersection. Anomalous chemical signatures in the water column and optical backscatter responses were observed in CTD stations 15 and 16 on the western portion of the rift valley. The valley floor is wider and intra-valley floor bathymetric highs are observed here. CTD 15 was located at the base of the western valley wall and CTD 16 on the valley floor on a linear high (Figure 1).

Methodology

Sampling strategy and technique

For the present study a 50 km long ridge segment between 05°54'N, 61°06'E and 05°38'N, 61°32'E was chosen for detailed water-column survey. Based on the high-resolution swath bathymetry (Figure 1) developed during our earlier cruise, SK-195 and hydrothermal anomalies reported in the cruise report² CD-149, we selected six CTD hydrocast locations along the rift valley. Two sampling locations CTD-15 (05°54'N, 61°13'E) and CTD-16 (05°54'N, 61°06'E) (proximal CTDs) were selected near the station WP-5 (06°03'N, 60°56'E), where maximum hydrothermal signatures were recorded by earlier authors³. To investigate the geochemical behaviour of laterally extended diffused plume, four distal stations CTD-17 (05°45.5'N, 61°21.6'E), CTD-14 (05°43.5'N, 61°27.5'E), CTD-20 (05°42.3'N, 61°29.1'E) and CTD-21 (05°38.3'N, 61°31.2'E) (Figure 1) were investigated in further south-east.

As the backscatter anomalies were recorded below 2400 m, we restricted our water sampling mainly in deep (>2000 m) water. A Seabird CTD system (SBE 9/11 plus), bottle rosette along with light scattering sensors (WET Labs 633 and 634) was used for water-column survey. Water samples were collected during CTD hydrocast using 10 l acid-washed, Teflon-coated Niskin water samplers. Based on the CTD and nephelometer profiles, duplicate water samples were collected for volatiles and trace-metal analysis.

Measurement of temperature anomalies

The hydrothermal potential temperature anomaly ($\Delta\theta$) was determined from the linear relationship⁸ between potential temperature (θ) and potential density (σ_θ).

Chemical analysis of water samples

After recovering the CTD on-board, sub-sampling for different geochemical parameters was performed immediately. On-board dissolved methane was analysed, but samples for helium isotopes and trace metals were collected and preserved for further analysis.

Helium isotopes: Sampling for helium isotope was done selectively based on temperature and optical backscatter profiles. Upon recovery of the CTD on-board, samples were collected and crimped within fresh copper tubes. Gas extraction and isotopic analysis for He^3 and He^4 were carried out with a dual-collector mass spectrometer at the Pacific Marine Environmental Laboratory, USA. The excess of helium-3 isotope in plume is expressed as $\delta^3\text{He} (\%) = (R_{\text{sample}}/R_{\text{atm}} - 1) \times 100$, where $R = [\text{He}^3]/[\text{He}^4]$ in water samples or atmosphere.

Dissolved methane: Dissolved gases were extracted from sea-water samples using ultrasonic vacuum degassing system⁹. Methane content in selected samples was measured on-board with a Carlo Erba CE 8000 Top Gas Chromatograph equipped with a FID.

Dissolved iron (DFe) and manganese (DMn): For dissolved trace metals, water samples were first filtered through 0.45 μm filter papers and then immediately acidified with ultra-pure nitric acid to maintain a pH ~ 2.0 . The preserved samples were returned to the shore-based laboratory for analysis. DFe was analysed using APDC-MIBK extraction, followed by Zeeman graphite furnace AAS (Perkin Elmer Analyst 600) measurements as described by Danielsson *et al.*¹⁰. DMn was similarly preconcentrated using SDDC-MIBK and analysed with GFAAS.

Particulate iron (PFe) and manganese (PMn): After filtration the filter papers were rinsed with distilled water, dried and kept in individual petri plates. In the shore-based laboratory the filter papers were digested with ultra pure perchloric (1.0 ml) and nitric acid (1.0 ml). Diluted samples were analysed for PFe using Flame AAS (Perkin Elmer Analyst 200) and for PMn with GFAAS.

Results and discussion

Optical and thermal anomalies

The optical backscatter signals (OBS) and thermal anomalies recorded during our present survey over CR were an order of magnitude lower than those of the CR-2003 event plume as reported earlier³. The two-dimensional contour for OBS (Figure 2b) developed with the dataset for six axial hydrocasts showed two distinct layers separated by hundreds of metres. The top layer between 2500 and 2900 m coincides with the CR-2003 plume layer, but the deeper one between 3100 and 3400 m has not been reported earlier. Both the layers are characterized with maximum backscatter intensity (about 0.1 V) at CTD-16 and CTD-15, close to the CR-2003 event source, WP-5 of Murton *et al.*³, which gradually drops further southeast. Distribution of water-column thermal signature (Figure 2a) also shows a similar feature with maximum potential temperature anomalies ($\Delta\theta$) around CTD-16 and CTD-15. The layering feature in nephelometric distribution (Figure 2b) did not appear in the temperature anomaly (Figure 2a) and that could be the result of rapid dissipation of heat compared to particulates during plume mixing. In particular, CTD-15 and CTD-16 had maximum $\Delta\theta$ of $0.012 \pm 0.002^\circ\text{C}$ between 3000 and 3200 m. This drops further south (Figure 2a) and in distal CTDs, there is hardly any thermal signature ($\Delta\theta < 0.003^\circ\text{C}$).

The heat content per unit volume (Q) corresponding to maximum $\Delta\theta$ measured using the relation¹¹, $Q = \rho C_p \Delta\theta$

was 50 ± 10.5 J/l. This is almost one-third of the average real-time heat content (139.0 J/l) record³. This result indicates that if the present observation is the residual effect of the earlier event plume, the heat content could have reduced due to dilution of the plume over time. Two plume layers as detected with backscatter signals also suggest the possibility of an alternate source, which could be continuous and needs to be investigated further.

Geochemistry of trace metals

Distribution of dissolved and particulate trace metals:

The depth distribution of dissolved and particulate fractions of Fe and Mn at CTD-16 has two distinct maxima (Figure 3). These coincide with two highs in the OBS contour. DMn in the shallow layer has wide variations (range between 4.2 and 10.7 nmol/l; av 5.4 ± 2.8 nmol/l) compared to the deeper one (range between 3.6 and

7.5 nmol/l; av 5.3 ± 1.4 nmol/l) within the turbid zone of CTD-15 and CTD-16. In diluted plume samples (CTD-14, CTD-17, CTD-20), DMn drops to 3.0 ± 0.64 nmol/l in the same depth range. Average DMn measured 1000 m above and below the plume depth was 1.9 ± 0.6 nmol/l, which is more than the typical Indian Ocean deep-water concentration (0.2–1.3 nmol/l)¹². DFe distribution in general follows the same pattern as DMn. Highest DFe was 11.7 and 9.05 nmol/l at 2700 and 3290 m respectively (Figure 3).

Occurrence of particulate metal peaks below those of the dissolved ones (Figure 3) indicates large-scale precipitation and separation of the particulates from the original non-buoyant layer due to which dissolved metals float on top. There is no such fractionation within the water column in the deeper plume, which obviously is a fresh one.

Particulate Fe forms a major fraction of total Fe (>60–97%; mean 82%). This high percentage of particulate iron in both the layers is comparable with other event plume records (PFe > 80% for event plumes and 50–60% for chronic discharge)¹ in the world oceans. It is important to note that there was hardly any PFe variation between the proximal and distal CTDs, while these differ significantly in PMn (Table 1). This is due to fast oxidation of Fe compared to Mn. Relatively less abundance of PFe and PMn in the deeper layer (Table 1) supports the conclusion that it was a fresh event.

Dissolved manganese to heat ratio: The DMn/heat ratio is a thermo-chemical property of a plume which is most useful for recognizing the plume type¹. An event plume differs from steady-state chronic emissions in terms of uniform manganese-to-heat ratio in near-field plume samples¹³. Our present observation revealed that the mean DMn/heat ratios at CTD-15 and CTD-16 (0.13 ± 0.06 nmol/J) agree well with those of event plumes found in East Pacific (0.15 nmol/J)^{14–16}. Murton *et al.*³ have reported this ratio as 0.08 ± 0.02 nmol/J during the CR-2003 event. Enhancement in this ratio in the present study suggests fast dissipation of heat compared to oxidative removal of Mn.

Fe/Mn ratio: It is interesting to note that the average DFe/DMn ratio in both the layers was close to unity (1.07 ± 0.3), and differed significantly from the previous record³ of 5.1 ± 0.07 mol/mol. Low Fe/Mn ratio (~ 1.0) is a characteristic feature of any chronic hydrothermal emission, but mega events are always associated with higher DFe/DMn (>2 mol/mol) ratio^{1,17}. This change in the DFe/DMn ratio is mostly due to fast oxidative removal of DFe relative to DMn. Thus in absence of continuous input, episodic mega event might lose its characteristics over a period of time. Thus, DFe/DMn signatures slowly become indistinguishable from the mature chronic plume. The ratio of metal particulates, e.g. PMn/PFe (~ 0.01 mol/mol), closely resembled those of the East Pacific events,

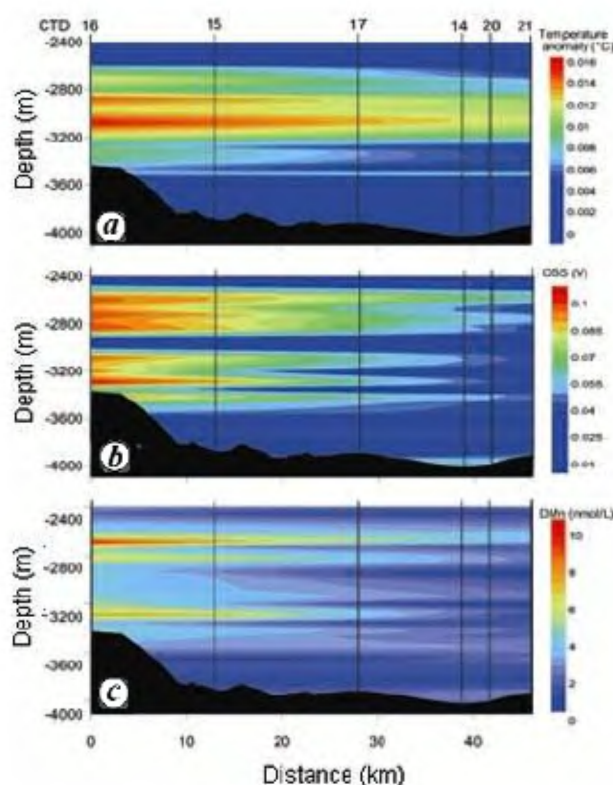


Figure 2. Two-dimensional transects of water column: (a) Potential temperature anomaly (°C); (b) optical backscatter signals (V) and (c) dissolved manganese (nmol/l) along the axial rift valley. The intense temperature anomaly was found as a broad band between 2850 and 3150 m, unlike two separate layers of DMn and optical backscatter signals appear between 2500–2900 m and 3100–3400 m. As density gradient limits the depth distribution of non-buoyant plumes, the DMn, plume particulates remain in suspension and slowly disperse horizontally over a distance¹⁶. The hydrothermal heat on the other hand, dissipates fast in all directions. Hence receiving heat from both the plumes, the intermediate (2850–3150 m) water mass would be expected to have maximum temperature anomaly.

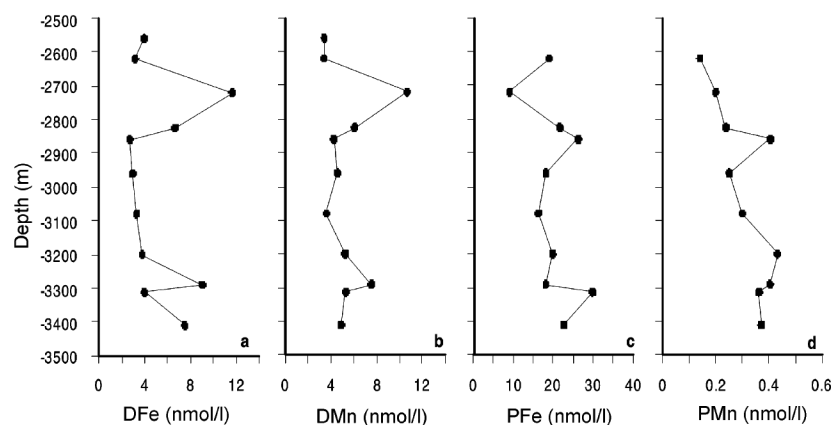


Figure 3. Vertical distribution of (a) dissolved iron, DFe, (b) dissolved manganese, DMn, (c) particulate iron, PFe and (d) particulate manganese, PMn in water column at CTD-16 (05°53.9'N, 61°06.3'E).

Table 1. Geochemical parameters associated with the two plume layers

Parameters	Depth range (m)	Proximal CTDs (stations 15 and 16)	Distal CTDs (stations 14, 17, 20, 21)
CH ₄ (nmol/l)	2560–2960	1.68 ± 0.36	2.25 ± 0.9
	3080–3400	2.08 ± 1.05	1.61 ± 0.56
CH ₄ /Mn (mol/mol)	2560–2960	0.43 ± 0.16	0.56 ± 0.14
	3080–3400	0.40 ± 0.18	0.75 ± 0.10
PFe (% of total)	2560–2960	82.0 ± 10.9	84.8 ± 11
	3080–3400	79.5 ± 8.6	81.8 ± 12
PMn (% of total)	2560–2960	8.9 ± 5.7	20.3 ± 9.2
	3080–3400	6.7 ± 1.1	18.5 ± 9.8
DFe/DMn (mol/mol)	2560–2960	0.93 ± 0.2	1.12 ± 0.5
	3080–3400	1.02 ± 0.3	1.65 ± 0.8
$\delta^3\text{He}$ (‰)	2560–2960	Not analysed	14.7
	3080–3400	26.07–31.01	13.6–13.85
Mn/heat (nmol/J)	2560–2960	0.13 ± 0.06	0.16 ± 0.07
	3080–3400	0.14 ± 0.08	0.08 ± 0.05

EP-96A (0.0082 mol/mol), EP-96B (0.0109 mol/mol), but differs from the Atlantic co-axial event (0.0021 mol/mol), in the Juande Fuca Ridge¹⁸.

Geochemistry of volatiles

Helium anomaly: High concentrations of dissolved volatiles, characteristic to hydrothermal emission (viz. methane and helium-3) were observed in water samples from the same depth ranges at CTD-15 and CTD-16. At CTD-16, within plume layers, especially samples from the plume core had higher volatile content. The deeper layer was relatively enriched with methane and helium-3. Excess of dissolved helium-3 expressed^{19,20} as $\delta^3\text{He}$, the best indicator of hydrothermal activity, had maximum range of 26.07–31.08‰ ($^3\text{He} = 7.6\text{--}7.9 \times 10^{-14} \text{ cm}^3 \text{ STP/g}$) at CTD-16 between 3200 and 3410 m. This maximum $\delta^3\text{He}$ was the second highest reported helium anomaly in the Indian Ocean, the highest being 33‰ near the RTJ (65°54.4'E, 19°29'S), Central Indian Ridge²¹. Although our results for $\delta^3\text{He}$ were sparse in the shallow plume, it

appeared depleted in helium-3 with a maximum value of $\delta^3\text{He} = 14.7\%$ ($^3\text{He} = 6.8 \times 10^{-14} \text{ cm}^3 \text{ STP/g}$) at 2800 m, slightly elevated relative to the background value of 13.3%. A striking enrichment of ^3He ($7.94 \times 10^{-14} \text{ cm}^3 \text{ STP/g}$) at the core of the deep plume layer further confirms that it is a relatively fresh event compared to the plume on top. The ratio $^3\text{He}/\Delta\theta$ in both layers exhibits major variations ranging from 6.0 to $9.1 \times 10^{-12} \text{ cm}^3 \text{ STP/g/}^\circ\text{C}$, much higher than that reported earlier for a typical event plume ($0.3\text{--}0.4 \times 10^{-12} \text{ cm}^3 \text{ STP/g/}^\circ\text{C}$)^{19,22}, but consistent with the mature chronic GR2-V12 plume over Gorda Ridge in the Pacific Ocean²³. This similarity in volatile-to-heat ratio can be attributed to a geochemical saturation/equilibrium phase during which hardly any change can be noticed, irrespective of the event or chronic sources. Water samples from CTD-14, CTD-17, CTD-20 and CTD-21 further southeast did not show any significant enrichment of ^3He with a mean $\delta^3\text{He}$ of 13.5%.

CH₄/Mn ratio: Methane concentrations at all the sampling locations varied between 1.0 and 3.0 nmol/l within the

plume layers. CH₄/Mn molar ratio showed minor variation (0.4–0.8 mol/mol) in that area, well within the range so far seen for an event discharge (0.1–1.0 mol/mol). In chronic hydrothermal field methane is mostly consumed by methylotrop²⁴, but the occasional cataclysmic mega event releasing voluminous solution within a short period of time is not expected to develop enough microbial activity to support methane oxidation. In such cases methane can persist in the water column and gets diluted in the far field away from the source. Observed degree of dilution was the same for both tracers, CH₄ and Mn. Marginal increase in CH₄/Mn molar ratio away from the source could be due to the removal of DMn through scavenging in particulates, as observed²⁵ in 12°41.6'N EPR.

Conclusion

The present observations show that even a year after an unusually large hydrothermal event, CR-2003 over CR, the plume components particularly dissolved iron, manganese, helium-3, and methane still persist within the water column. Certain tracers revealed one non-buoyant plume layer laterally expanded further southeast. We also found another layer characterized with typical hydrothermal components near the valley floor. The heat content per unit volume as well as %PFe, Mn/heat and CH₄/Mn ratios indicate that there was small-scale emission(s) following the major event, CR-2003. Further detailed investigation around this area is needed to establish a better understanding of plumes found during the present study. Thus we conclude that the event plume, CR-2003 and events following it had a major influence on the water-column characteristics in that area.

- Massoth, G. J. *et al.*, Manganese and iron in hydrothermal plumes resulting from the 1996 Gorda Ridge Event. *Deep Sea Res. II*, 1998, **45**, 2683–2712.
- Anon., Cruise report of RSS Charles Darwin (CD-149) (18 July–6 August 2003), Southampton Oceanography Centre, UK, p. 3.
- Murton, J. B., Baker, E. T., Sands, C. M. and German, C. R., Detection of an unusual large hydrothermal event plume above the slow spreading Carlsberg Ridge, NW Indian Ocean. *Geophys. Res. Lett.*, 2006, **33**, 1–5.
- Fournier, M., Patriat, P. and Leroy, S., Reappraisal of the Arabia–India–Somalia triple junction kinematics. *Earth Planet. Sci. Lett.*, 2001, **189**, 103–114.
- Chaubey, A. K., Bhattacharya, G. C., Murty, G. P. S. and Desa, M., Spreading history of the Arabian Sea: Some new constraints. *Mar. Geol.*, 1993, **112**, 343–352.
- Ramana, M. V., Ramprasad, T., Kamesh Raju, K. A. and Desa, M., Geophysical studies over a segment of the Carlsberg Ridge, Indian Ocean. *Mar. Geol.*, 1993, **115**, 21–28.
- Kamesh Raju, K. A., Kodagali, V. N. and Fujimoto, H., In Proceeding of 35th Annual Convention of the Indian Geophysical Union, National Institute of Oceanography, Goa, 1998, pp. 29–30.
- Baker, E. T. and Massoth, G. J., Characteristics of hydrothermal plumes from two vent fields on the Juan de Fuca Ridge, northeast Pacific Ocean. *Earth Planet. Sci. Lett.*, 1987, **85**, 59–73.
- Schmitt, M., Faber, E., Botz, R. and Stoffers, P., Extraction of methane from sea water using ultrasonic vacuum degassing. *Anal. Chem.*, 1991, **5**, 529–532.
- Danielsson, L. G., Magnusson, B. and Westerlund, S., An improved metal extraction procedure for the determination of trace metals in sea water by atomic absorption spectrometry with electro thermal atomization. *Anal. Chim. Acta*, 1978, **98**, 47–57.
- Bischoff, J. L. and Rosenbauer, R. J., An empirical equation of state for hydrothermal sea water (3.2 per cent NaCl). *Am. J. Sci.*, 1985, **285**, 725–763.
- Saager, P. M., De-Baar, H. J. W. and Burkill, P. H., Manganese and iron in Indian Ocean waters. *Geochim. Cosmochim. Acta*, 1989, **53**, 2259–2267.
- Chin, C. S., Coale, K. H., Elrod, V. A., Johnson, K. S., Massoth, G. J. and Baker E. T., *In situ* observations of dissolved iron and manganese in hydrothermal vent plumes, Juan de Fuca Ridge. *J. Geophys. Res. B*, 1994, **99**, 4969–4984.
- Massoth, G. J. *et al.*, Temporal and spatial variability of hydrothermal manganese and iron at Cleft segment, Juan de Fuca Ridge. *J. Geophys. Res.*, 1994, **99**, 4905–4923.
- Massoth, G. J. *et al.*, Observations of manganese and iron at the co-axial seafloor eruption site, Juan de Fuca Ridge. *Geophys. Res. Lett.*, 1995, **22**, 151–154.
- Baker, E. T., Patterns of event and chronic hydrothermal venting following a magmatic intrusion: New perspectives from the 1996 Gorda Ridge eruption. *Deep Sea Res.-II*, 1998, **45**, 2599–2618.
- Baker, E. T., Massoth, G. J. and Feely, R. A., Cataclysmic hydrothermal venting on the Juan de Fuca Ridge. *Nature*, 1987, **329**, 149–151.
- Feely, R. A., Baker, E. T., Lebon, G. T., Gendron, J. F., Massoth, G. J. and Mordy, C. W., Chemical variations of hydrothermal particles in the 1996 Gorda Ridge Event and chronic plumes. *Deep Sea Res.-II*, 1998, **45**, 2637–2664.
- Lupton, J. E., Hydrothermal plumes: Near and far field. In *Sea Floor Hydrothermal Systems: Physical, Chemical, Biological and Geological Interactions* (eds Humphris, S. E. *et al.*), Geophysical Monograph, American Geophysical Union, Washington, D.C., 1995, vol. 91, pp. 317–346.
- Lupton, J. E., Hydrothermal helium plumes in the Pacific Ocean. *J. Geophys. Res.*, 1998, **103**, 15853–15868.
- Jean-Baptiste, P., Mantsi, F., Pauwells, H., Grimaud, D. and Patriat, P., Hydrothermal 3-He and manganese plume at 19°29'S on the Central Indian Ridge. *Geophys. Res. Lett.*, 1992, **19**, 1787–1790.
- Lupton, J. E., Baker, E. T. and Massoth, G. J., Variable ³He/heat ratios in submarine hydrothermal systems: Evidence from two plumes over the Juan de Fuca ridge. *Nature*, 1989, **337**, 161–169.
- Kelley, D. S., Lilley, M. D., Lupton, J. E. and Olson, E. J., Enriched H₂, CH₄ and ³He concentrations in hydrothermal plumes associated with the 1996 Gorda Ridge eruptive event. *Deep Sea Res.-II*, 1998, **45**, 2665–2682.
- Baross, J. A., Lilley, M. D. and Gordon, L. I., Is the CH₄, H₂ and CO venting from submarine hydrothermal systems produced by thermophilic bacteria? *Nature*, 1982, **298**, 366–368.
- Charlou, J. L., Bougault, H., Appriou, P., Jean-Baptiste, P., Etoubleau, J. and Birolleau, A., Water column anomalies associated with hydrothermal activity between 11°40' and 13°N on the East Pacific Rise: Discrepancies between tracers. *Deep Sea Res.-I*, 1991, **38**, 569–596.

ACKNOWLEDGEMENTS. We thank Dr S. R. Shetye, Director, National Institute of Oceanography, Goa and Dr V. P. Dimri, Director, National Geophysical Research Institute, Hyderabad for their interest and continuous support. We also thank Dr John Lupton, Mr Ron Green and Mr Leigh Evans for analysing water samples for helium isotopes at the Helium Isotope Laboratory, NOAA/PMEL, Oregon, USA. The Ministry of Earth Sciences, New Delhi is thanked for providing ship time of ORV Sagar Kanya. Thanks are also due to the crew on-board ORV Sagar Kanya for help during deep-sea sampling. This is NIO contribution no. 4393.

Received 27 December 2007; revised accepted 18 June 2008